Active Clamp Forward Converter With a New Switch Control Technique for Reducing Transient Voltage Overshoot

Dae-Hun Kown[1] and Jae-Kuk Kim[1]

[1] Department of Electrical Engineering, Inha University, Republic of Korea

Abstract—**An active clamp forward converter is popular in low- and medium-power applications. However, due to the voltage overshoot on the clamp capacitor in the transient state, the switches can suffer from high voltage stress, causing the adoption of higher voltage-rated switches and threatens system stability. This article proposes a new switch control technique to reduce the voltage overshoot. The overshoot occurs as the clamp capacitor voltage increases when the transformer primary current flows to clamp capacitor. Thus, to block voltage increase during the corresponding interval, the proposed technique reduces clamp capacitor current by bypassing transformer current to the main switch. For bypass operation, main switch operates as a current source by decreasing gate-to-source voltage. Because the bypass operation does not change voltage gain between input and output, the proposed technique can alleviate the overshoot without affecting the feedback controller designs. To verify the effectiveness, a 300 W prototype is experimented.**

Index Terms— **Active clamp forward (ACF) converter, transient state, voltage overshoot, voltage stress.**

Fig. 1. Circuit diagram of the ACF converter.
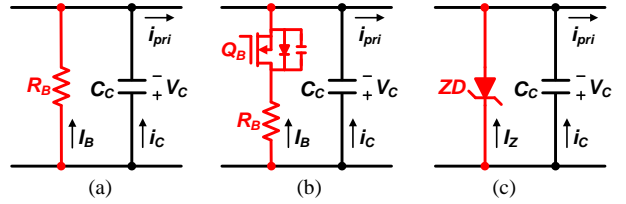
Fig. 2. Candidates that can be adopted considering the transient voltage overshoot of the ACF converter. (a) Resistor. (b) Resistor with a power MOSFET. (c) Zener diode.

I. INTRODUCTION

The active clamp forward (ACF) converter, shown in Fig. 1, is widely used in low- and medium-power applications [1]–[4]. It features simple structure and high efficiency, and the primary switches, Q_M and Q_A, have clamped voltage stress which is the sum of the input voltage V_{IN} and clamp capacitor voltage V_C. However, owing to the transient behavior, such as the transient voltage overshoot on the clamp capacitor C_C during a load transient, the switches can suffer from high voltage stress. The overshoot can cause even higher voltage stress than that in the steady state [5], consequently causing the adoption of higher voltage-rated switches and threatening the system stability.

To reduce the voltage stress on the switches of the ACF converter, many studies have been conducted [6]–[13]. By employing additional high-voltage-rated switches or diodes, they have reduced the voltage stress on the switches and improved the performance in the steady state. However, the use of additional high-voltage-rated semiconductors can increase the overall cost and volume. Furthermore, the voltage overshoot can still be a problem even in these approaches because they focus on the improvement in the steady state. In [14], regarding the transient operation, some solutions are described: adopting higher voltage-rated switches, decreasing the maximum duty ratio limit of Q_M and control bandwidth. While adopting higher voltage-rated switches can increase the

voltage margin, they have low performance and high cost in general. Decreasing the maximum duty ratio limit and control bandwidth can mitigate the overshoot, however, the dynamic performance on the output voltage can be degraded as a trade-off [14].

Basically, the voltage overshoot occurs as V_C increases when the transformer primary current i_{pri} flows to the clamp capacitor. Thus, as the approaches to relieve the overshoot, bypassing i_{pri} that flowing through C_C to another current path can be considered as shown in Fig. 2(a) and (b). The bypassing path can be easily made by adding a resistor, as shown in Fig. 2(a), which structure is the same as the RCD-snubber for clamping the voltage stress in the forward or flyback converters [15]–[18]. However, since the resistor dissipates the stored energy in C_C during the steady state as well as the transient state, it cannot be adopted considering the aim of the active clamp circuit, C_C and Q_A [1]. To activate the bypass circuit only in the transient state, the circuit can be modified by employing a power MOSFET as shown in Fig. 2(b). Through the control of the additional switch, the bypass circuit can be activated only in the transient state, which results in a reduction of the overshoot without degrading the conversion efficiency in the steady state. Meanwhile, in [19] and [20], the use of the zener diode to clamp the

TABLE I
COMPARISON WITH THE CANDIDATES SHOWN IN FIG. 2

|	Candidate 1 (Fig. 2(a))	Candidate 2 (Fig. 2(b))	Candidate 3 (Fig. 2(c))	Proposed Method
Performance (Steady State)	Fair	Good	Good	Good
Additional Cost	Low	High	High	Low
Flexibility	High	High	Low	High

Fig. 3. Load transient waveforms of the ACF converter.

(a)

(b)

Fig. 4. Key waveforms of the ACF converter in the conventional method. (a) During the steady state. (b) During the transient state.

voltage stress on the switch has been described. Similarly, it can be employed to the ACF converter to clamp the voltage stress by connecting it in parallel to C_C as shown in Fig. 2(c). While the approaches, shown in Fig. 2(b) and (c), can reduce the voltage overshoot, the additional components can suffer from high voltage stress in high-input-voltage applications where the input voltage is around 400 V, which can increase overall cost. Furthermore, to prevent the clamping operation by the zener diode in the steady state, the zener voltage should be higher than V_C in the steady state, however, there are few high-voltage-rated zener diodes. Therefore, this approach has low flexibility in high-input-voltage applications.

In order to reduce the voltage overshoot without additional high-voltage-rated components, this article proposes a new switch control technique. The concept of the proposed technique is the same as the approach shown in Fig. 2(b), but it bypasses i_{pri} to Q_M. During the bypass, Q_M and Q_A are on state, and Q_M operates as a current source by decreasing the gate-to-source voltage. To decrease the gate-to-source voltage, the gate driver of Q_M is simply modified, which hardly affects the overall cost and volume. Moreover, since the bypass operation does not change the overall feedback control loop, the proposed technique can alleviate the voltage overshoot without affecting dynamic performance on the output voltage.

Table I illustrates the comparison of the above-mentioned approaches and the proposed method on various aspects. First, since the proposed method changes the operational state to reduce the overshoot only in the transient state, it has the same performance with the conventional method in the steady state. Second, there is few increases of the cost and no limitations according to the applications owing to the absence of additional high-voltage-rated semiconductor. Finally, the design of the proposed technique can be conducted flexibly because it is conducted just by changing the operational state of Q_M. As a result, the proposed method can have advantages compared to the approaches shown in Fig. 2.

The detailed operation, design procedures, and experimental results are presented in the following sections.

II. CONVENTIONAL AND PROPOSED METHODS

A. Conventional Method

Fig. 3 shows the load transient waveform of the ACF converter, where V_{SEN} is the sum of V_{IN} and V_C, and Fig. 4 shows the key waveforms of the ACF converter in the conventional method during steady state and transient state
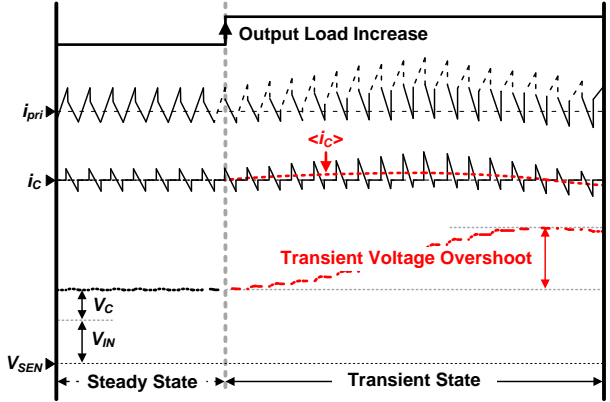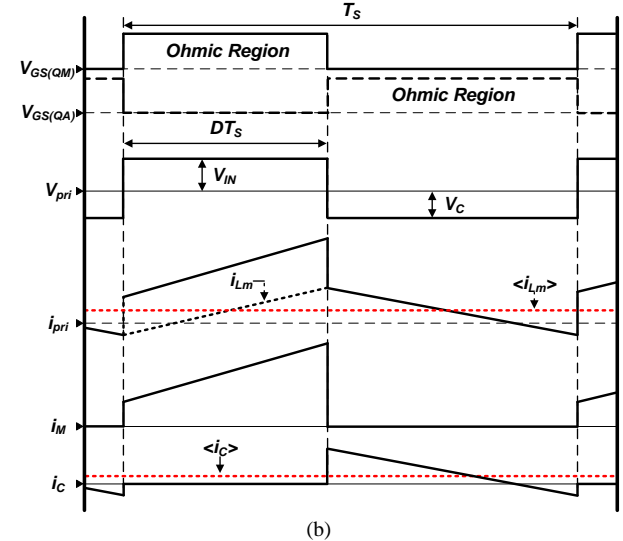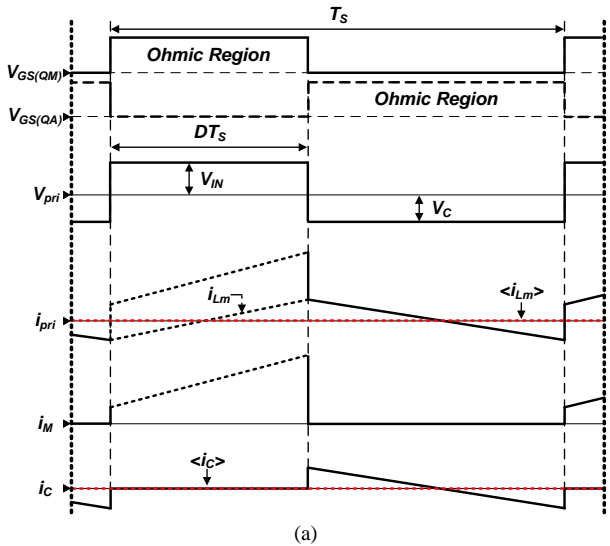
when V_{SEN} is increasing in Fig. 3, where $V_{GS(QM)}$ and $V_{GS(QA)}$ are the gate-to-source voltages of the switches, V_{pri} is the voltage across the magnetizing inductor L_m, i_M is the current of Q_M, and D is the duty ratio of Q_M. In both conditions in Fig. 4, there are two operational states according to the switching state of Q_M in equal. When Q_M

is tuned-on, V_{IN} is applied to L_m, and input powers to the output. After turning-off Q_M, Q_A is turned-on, and i_{pri} becomes to the magnetizing current i_{Lm} and flows to C_C. In this state, the clamp capacitor resets the transformer, and there is no power delivering to the output.

However, even though the control of the switches is the same, there are differences in the voltage and current waveforms, as shown in Figs. 3 and 4. In the steady state, the current-second product of the clamp capacitor is balanced, i.e., the average current of the clamp capacitor $\langle i_C \rangle$ is zero in a switching period T_S. Thus, V_C and the voltage stress on the switches, V_{SEN}, are maintained at constant values as shown Fig. 3. However, after the load transition, the current-second balance of C_C has broken, i.e., $\langle i_C \rangle$ becomes positive as shown in Figs. 3 and 4(b). As a results, V_C starts to increase, and consequently it causes the transient voltage overshoot which increases the voltage stress of the switches.

In order to mitigate the overshoot, $\langle i_C \rangle$ should be decreased since V_C increases as $\langle i_C \rangle$ becomes positive. Reducing the average current can be achieved by bypassing i_{pri} to the other path, not to C_C, as shown in Fig. 2. However, as above-mentioned, the adoption of the additional components can be an undue burden on the cost of the ACF converter in high-input voltage applications.

B. Proposed Method

To improve the voltage overshoot without additional high-voltage-rated semiconductor, the new switch control technique is proposed in this paper. The concept of the proposed technique is shown in Fig. 5. In the conventional method, the current of the clamp capacitor i_C flows when Q_M is turned-off. However, the proposed technique bypasses i_{pri} to Q_M by operating as a current source to reduce the current flows through C_C during a period where Q_M is off state in the conventional method. Since the MOSFET operates as the current source in the saturation region, the operational state in Fig. 5 can be implemented by decreasing the gate-to-source voltage of Q_M [21]. During the state, the bypass current I_B can be defined as follows:

$$I_B = g_m (V_{GS(QM)} - V_{th(on)}) \tag{1}$$

where g_m is the transconductance, and $V_{th(on)}$ is the turn-on threshold voltage.

From (1), it can be noticed that I_B is determined by the gate-to-source voltage when Q_M operates as the current source. Thus, to operate Q_M as the current source and make I_B as a desired value, the gate-to-source voltage of Q_M should be adjusted. To adjust the gate-to-source voltage, the gate driver of Q_M is only and simply modified by adding a resistor R_X and small signal MOSFET Q_X as shown in Fig. 6, where V_{CC} is the gate driving voltage, R_G is the gate resistor. In the modified gate driver, when the gate signals of both switches become high signal, Q_M can operate as the current source by decreasing $V_{GS(QM)}$ as following:

$$V_{GS(QM)} = \frac{V_{CC} R_X}{R_G + R_X}. \tag{2}$$
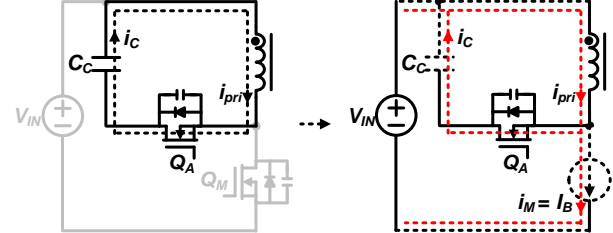
Fig. 5. Concept of the proposed technique.
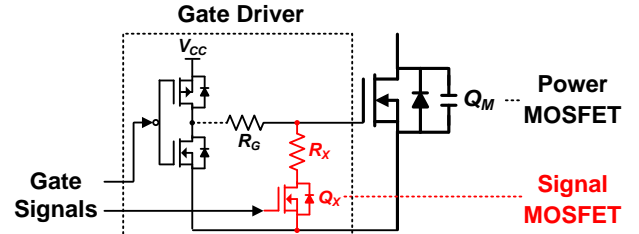
Fig. 6. Circuit diagram of the gate driver of Q_M for the proposed method.


(a)

(b)
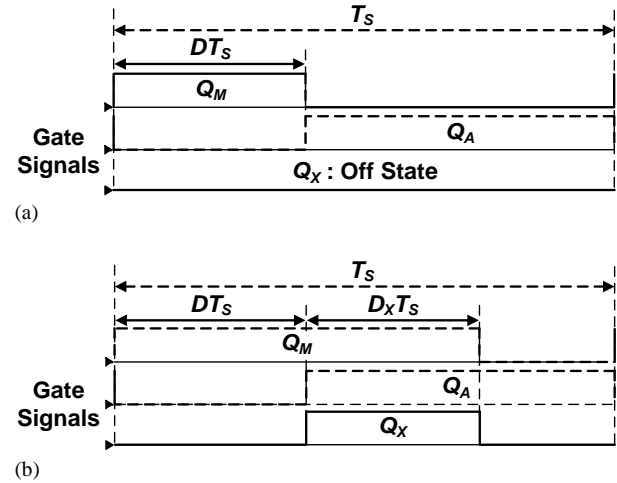
Fig. 7. Gate signals of the switches in the proposed method. (a) Conventional operation in the steady state. (b) Proposed operation in the transient state.

Fig. 7 shows the gate signals of the switches of the proposed method. Since the bypass operation is not required in the steady state, the proposed method adopts two operational modes. In the steady state, the proposed method controls switches, Q_M and Q_A, the same as the conventional method. Accordingly, Q_X maintains off state as shown in Fig. 7(a). On the contrary, the proposed technique is applied in the transient state. For the bypass operation, the turn-on signal of Q_M is extended and Q_X is turned-on for the extended interval, $D_X T_S$, to operate Q_M in the saturation region as shown in Fig. 7(b).

Fig. 8 shows the key waveforms of the proposed method in the transient state, which has three operational states according to the operational state of Q_M. While the two operational states, when Q_M operates in the ohmic region and is in the off state, are the same as the conventional operation, Q_M operates in the saturation region and bypasses i_{pri} for the additional operational state, $D_X T_S$, as shown in Fig. 8. As a result, $\langle i_C \rangle$ can be decreased
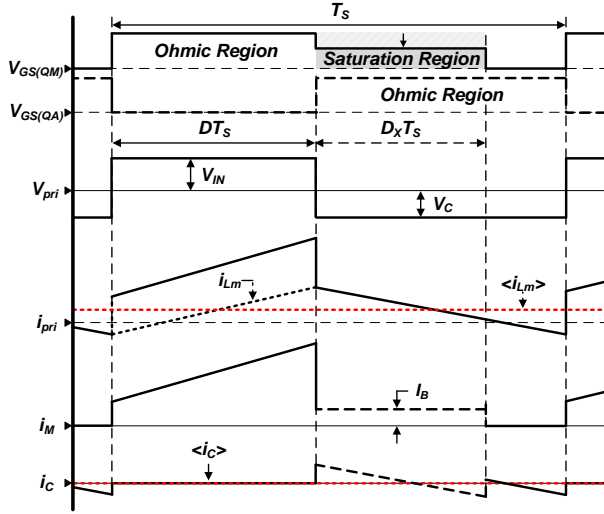
Fig. 8. Key waveforms of the ACF converter in the proposed operation.

compared to conventional method as shown in Figs. 4(b) and 8, which cause reduction of the transient voltage.

III. DESIGN PROCEDURES

The proposed method changes the operational modes in the transient state. This section presents the criteria for determining the transient state, the detailed control scheme, and design procedures of the proposed operation.

A. Detection of Transient Behavior and Control Scheme

In the steady state, the operation of the proposed method is identical to that of the conventional method. However, in the transient state, the proposed method adopts the new switch control technique to mitigate the voltage overshoot. Thus, to define the operational mode, the proposed method should detect the transient behavior. The transient behavior can be detected by measuring V_{SEN} because V_{SEN} is maintained at a constant value during the steady state and increases after the load transition as shown in Fig. 3. Therefore, by setting the threshold voltage V_{th} and comparing V_{SEN} with V_{th}, the transient state can be detected. Considering the voltage overshoot on C_C, this article determines V_{th} as follows:

$$V_{th} = V_{IN} + 1.1 V_C \qquad (3)$$

where the components in (3) are the input and clamp capacitor voltages when V_{SEN} is the maximum value in the steady state. As a results, V_{th} is always higher than V_{SEN} in the steady state, and the adoption of the proposed technique can be prevented.

Fig. 9 shows the control block diagram of the proposed method. It measures the output voltage V_O to control the output voltage and V_{SEN} to define the operational modes. The voltage controller outputs D as a control signal to regulate the output voltage to a reference voltage V_{REF}, and the operational mode is determined by comparing V_{SEN} with V_{th}. When V_{SEN} is lower than V_{th}, the comparator CMP outputs low signal, and the converter operates the same as the conventional ACF converter. On the other hand, as V_{SEN} is over V_{th} in the transient state, the output of CMP becomes high, and the operational mode is converted to the proposed operation with the change of the gate signals, as
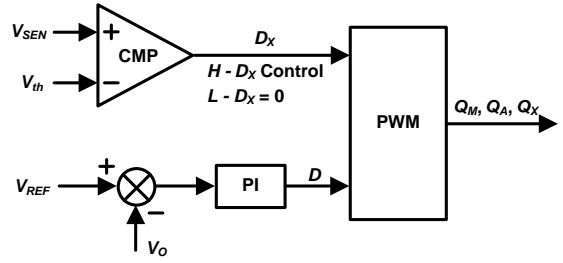
Fig. 9. Control block diagram of the proposed method.

shown in Fig. 7. In the proposed operation, Q_M bypasses I_B to reduce $<i_C>$, and the gate signal of Q_M is determined by D and D_X, and Q_X is controlled by D_X. Thus, I_B and D_X should be defined before applying the proposed operation, which is described in Section III. B.

B. Design of the Proposed Operation

As shown in Figs. 4 and 8, after turning-on Q_A, i_{pri} becomes to i_{Lm}, and the difference between i_{pri} and i_M flows to C_C. Thus, the relationship between i_{Lm} and i_M can be presented as

$$C_C \frac{dV_C}{dt} = < i_C > = < i_{Lm} > (1-D) - \int_{DT_S}^{T_S} i_M dt \qquad (4)$$

where $<i_{Lm}>$ is the average current of i_{Lm} during a switching cycle. In the conventional operation, since i_M is zero when Q_A is conducted as shown in Fig. 4, the equation (4) can be expressed as

$$C_C \frac{dV_C}{dt} = < i_{Lm} > (1-D). \qquad (5)$$

On the other hand, the proposed operation bypasses i_{pri} to Q_M for $D_X T_S$, hence, the equation (4) can be rewritten as follows:

$$C_C \frac{dV_C}{dt} = < i_{Lm} > (1-D) - I_B D_X. \qquad (6)$$

From (5) and (6), it can be noticed that the proposed operation reduces $<i_C>$, and its performance is determined by $I_B D_X$. Thus, it is defined first, and then, the design of each component is conducted in this article.

1) Design of $I_B D_X$: To suppress the voltage overshoot, $I_B D_X$ can be designed to have large value, however, it causes the large additional energy loss on Q_M, $E_{LOSS(QM)}$, during the bypassing operation, which can be calculated as

$$E_{Loss(QM)} = V_{th} I_B D_X T_S. \qquad (7)$$

On the other hand, when $I_B D_X$ is designed too small, there is few improvements in the overshoot. Considering this trade-off, $I_B D_X$ is designed to the average value of the maximum $<i_C>$, $<i_{Lm}>(1-D)$, and it can be obtained by substituting each component as following:

$$I_B D_X = \frac{2}{\pi} < i_{Lm} >_{max} (1 - D_{limit}) \qquad (8)$$

where $<i_{Lm}>_{max}$ is the maximum value of $<i_{Lm}>$, D_{limit} is the control duty ratio limit of Q_M, and $2/\pi$ is the coefficient to make the average value because the trajectory $<i_C>$ can be considered to have a sinusoidal envelope during the transient condition [5].

2) Design of I_B and D_X: In (8), since D_X can be controlled from zero to $(1-D)$, I_B is designed to $<i_{Lm}>_{max}$ in this article. As a result, D_X is determined as following:

TABLE II
EXPERIMENTAL COMPONENTS

Parameter		Components List
Primary Side	Switch	Q_M, Q_A IPP80R450P7
		Q_X 2N7000
	Clamp Capacitor (C_C)	470 nF
Transofmer	Core	PQ3220S(PL-9)
	Inductance (L_m)	800 µH
	Turns Ratio ($N_P : N_S$)	21 : 2
Secondary Side	Diode (D_1, D_2)	STPS61H100CWY
	Output Inductor (L_O)	30 µH
	Output Capacitor (C_O)	470 µF

$$D_X = \frac{2}{\pi}(1 - D_{limit}). \tag{9}$$

During the transient state, $<i_{Lm}>_{max}$ can be obtained by considering the peak magnetic flux density of the transformer, B_{PK}, which is expressed as

$$B_{PK} = \frac{L_m i_{Lm(PK)}}{A_e N_P} \tag{10}$$

where $i_{Lm(PK)}$ is the peak current of L_m, A_e is the effective area of the transformer core, and N_P is the turns of the primary side. Since the voltage across L_m is the input voltage during DT_S as shown in Figs 4 and 8, $i_{Lm(PK)}$ can be presented using the average value and current ripple as follows:

$$i_{Lm(PK)} = <i_{Lm}>_{max} + \frac{V_{IN}D_{limit}T_S}{2} = I_B + \frac{V_{IN}D_{limit}T_S}{2}. \tag{11}$$

Accordingly, the equation (10) can be presented based on I_B by applying (11) as following:

$$I_B = \frac{2B_{PK}A_e N_P - V_{IN}D_{limit}T_S}{2L_m}. \tag{12}$$

By designing D_X and I_B based on (9) and (12), the proposed method can alleviate the transient voltage overshoot because the design of the proposed operation is conducted considering the worst case.

IV. EXPERIMENTAL RESULTS

To verify the effectiveness of proposed method, a prototype operating at 70 kHz has been implemented with a 400 V input and 12 V/300 W output. The detailed experimental components are presented in Table II.

Fig. 10 shows the experimental results of the ACF converter in the steady state at 10 % and full load conditions in the proposed method. As can be seen from the waveforms, the operation in the steady state is the same as the conventional one, hence, there is no performance degradation in the steady state. Since the operation at the full load condition is the worst case, the design of the
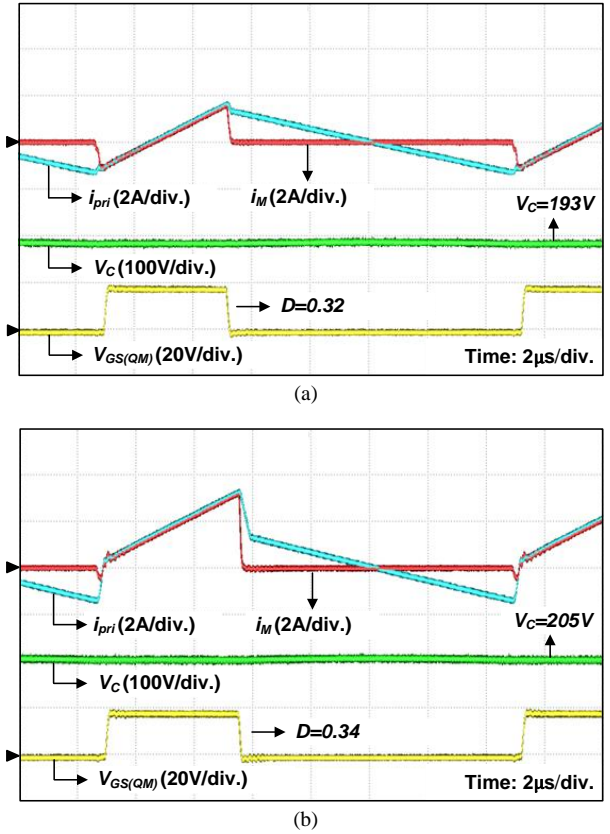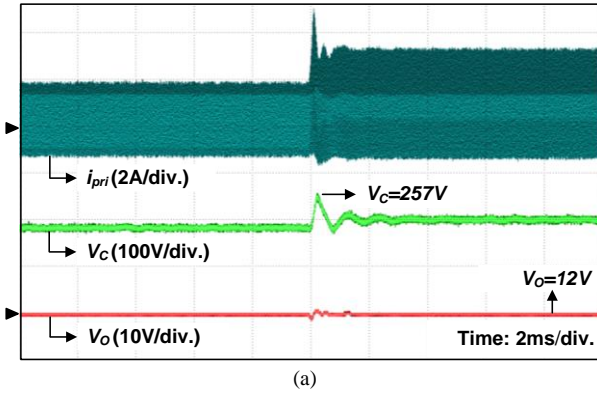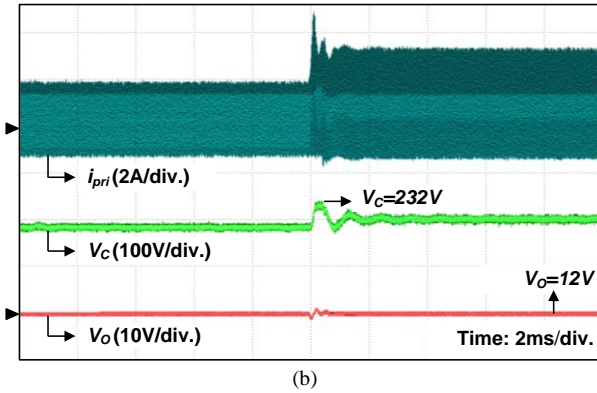

Fig, 10. Experimental results of the ACF converter in the steady state. (a) 10 % load condition. (b) Full load condition

proposed operation is conducted based on the experimental results in Fig. 10(b). From (3), the threshold voltage V_{th} is determined as 625 V by giving a 10 % of V_C to V_{SEN} in the worst case. The remaining two design components can be defined based on (9) and (12). As the core of the transformer is selected to PQ32320S, the components in (12) related to the core parameter are determined to $Ae = 170 \text{ mm}^2$ and $B_{PK} = 0.36 \text{ T}$ which is value in the worst case. The control duty ratio limit on Q_M, D_{limit}, is selected to be 0.4 considering the operation in the worst case. Accordingly, the equations (9) and (12), D_X and I_B, are calculated to about 0.4 and 0.2. To make a 0.2 A of I_B, $V_{GS(QM)}$ is determined to be 3.7 V and the gate resistor R_G and additional resistor R_X are selected as 18 Ω and 5 Ω at 17 V V_{CC}, respectively. Moreover, a small signal MOSFET, 2N7000, is adopted for Q_X, hence, there is no additional high-voltage-rated semiconductors. Therefore, the proposed method hardly affects the overall cost and volume.

Fig. 11 shows the experimental results of the load transient from 10 % to full load conditions with 0.06 A/µs slew rate when the conventional method and proposed method are applied respectively. As shown in Fig. 11, there are very little differences in both waveforms, except for V_C. The difference of V_C comes from the changes in the operational mode. The proposed method changes the operational mode when V_C is over 225 V, i.e., V_{SEN} is over 625 V, and reduces the overshoot by bypassing i_{pri} to Q_M. As a results, the proposed method has lower overshoot than the conventional method. However, since the overall

(a)

(b)

Fig, 11. Experimental results of the load transient from 10 % to full load conditions. (a) Conventional method. (b) Proposed method.
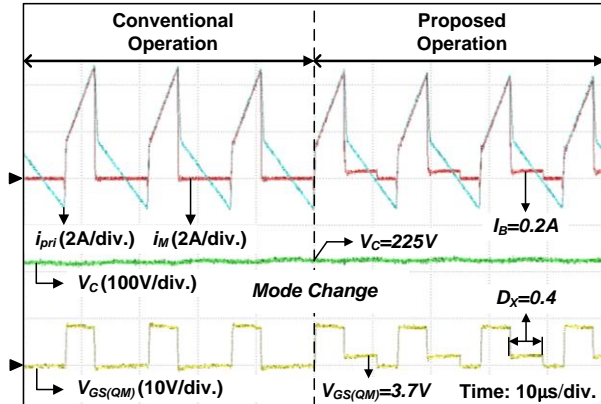

Fig. 12. Extended waveforms of Fig. 11(b) when the operational mode is changed into the proposed operation.

feedback control loop is the same, the other waveforms except for V_C have almost the same trajectories in both methods.

Fig. 12 shows the extended waveforms of Fig. 11(b) when the operational state is changed to the proposed operation in the proposed method. When V_C is over 225 V, the proposed method changes the operational mode to the proposed operation, and the bypass operation is conducted as shown in Fig. 12. As a results, $<i_C>$ can be reduced which leads to the reduction of voltage overshoot.

In this article, the overall explanations, experiments, and the design procedures are described based on the load transient behavior because the overshoot is larger in the load transient than in the line transient [5]. However, since the overshoot occurs on C_C equally in the line transient

condition, the proposed method can be applied in the same way to the line transient condition. Thus, the proposed method can mitigate the voltage overshoot under the entire operating conditions.

V. CONCLUSION

A new switch control technique for reducing the transient voltage overshoot of the ACF converter was proposed. The proposed technique mitigates the overshoot by bypassing the transformer current that flows to the clamp capacitor to the main switch. For the bypass operation, the main switch operates as the current source by decreasing the gate-to-source voltage. To decrease the gate-to-source voltage, the gate driver of Q_M is simply modified, which hardly increases overall cost. Moreover, since the bypass operation does not change the overall feedback control loop, the proposed technique can alleviate the voltage overshoot without affecting the feedback controller designs. The experimental results show the effectiveness of the proposed method.

REFERENCES

[1] F. D. Tan, "The forward converter: From the classic to the contemporary," in *Proc. IEEE APEC*, Mar. 10–14, 2002, vol. 2, pp. 857–863.

[2] H. Wu and Y. Xing, "Families of forward converters suitable for wide input voltage range applications," *IEEE Trans. Power Electron.*, vol. 29, no. 11, pp. 6006–6017, Nov. 2014.

[3] S. S. Lee, S. W. Choi, and G. W. Moon, "High-efficiency active-clamp forward converter with transient current build-up (TCB) ZVS technique," *IEEE Trans. Ind. Electron.*, vol. 54, no. 1, pp. 310–318, Feb. 2007.

[4] H. Wu and Y. Xing, "Families of forward converters suitable for wide input voltage range applications," *IEEE Trans. Power Electron.*, vol. 29, no. 11, pp. 6006–6017, Nov. 2014.

[5] Q. Li, F. C. Lee, and M. M. Jovanovic, "Large-signal transient analysis of forward converter with active-clamp reset," *IEEE Trans. Power Electron.*, vol. 17, pp. 15–24, Jan. 2002.

[6] K. B. Park, C. E. Kim, G. W. Moon, and M. J. Youn, "Multi-level active clamp forward converter with reduced voltage stress," in *Proc. IEEE Power Electron. Spec. Conf.*, 2008, pp. 938–943.

[7] J. K. Kim, W. S. Oh, and G. W. Moon, "A novel two-switch active clamp forward converter for high input voltage applications," in *Proc. IEEE Power Electron. Spec. Conf.*, Jun. 2008, pp. 3028–3034.

[8] K. B. Park, C. E. Kim, G. W. Moon, and M. J. Youn, "Three-switch active clamp forward converter with low switch voltage stress and wide ZVS range for high-input-voltage applications," *IEEE Trans. Power Electron.*, vol. 25, no. 4, pp. 889–898, Apr. 2010.

[9] K. B. Park, G. W. Moon, and M. J. Youn, "Series-input series-rectifier interleaved forward converter with a common transformer reset circuit for high-input-voltage applications," *IEEE Trans. Power Electron.*, vol. 26, no. 11, pp. 5209–5216, Nov. 2011.

[10] C. E. Kim, J. B. Lee, J. I. Baek, H. S. Youn, and G. W. Moon, "Improved three switch-active clamp forward converter with low switching and conduction losses," *IEEE Trans. Power Electron.*, vol. 34, no. 6, pp. 3242–3253, Jun. 2019.

[11] M. H. Kim, S. Lee, B. Lee, J. Kim, and J. Kim, "Double-ended active-clamp forward converter with low DC offset current of transformer," *IEEE Trans. Ind. Electron.*, vol. 67, no. 2, pp. 1036–1047, Feb. 2020.

[12] S. H. Lee, B. Lee, D. Kwon, J. Ahn, and J. Kim, "Two-mode low-voltage DC/DC converter with high and wide input voltage range," *IEEE Trans. Ind. Electron.* vol 68, no. 12, pp. 12088–12099, Dec. 2021.

[13] S. H. Lee, D. Kwon and, J. Kim, "Variable duty control in two-mode LDC for soft-change at the mode transient," *IEEE Trans. Ind. Electron.*, vol. 70, no. 1, pp. 364–372, Feb. 2022.

[14] Q. M. Li and F. C. Lee, "Design consideration of the active-clamp forward converter with current mode control large-signal transient," *IEEE Trans. Power Electron.*, vol. 18, no. 4, pp. 958–965, Jul. 2003.

[15] A. Abramovitz, T. Cheng, and K. Smedley, "Analysis and design of forward converter with energy regenerative snubber," *IEEE Trans. Power Electron.*, vol. 25, no. 3, pp. 667–676, Mar. 2010.

[16] A. Abramovitz, C. S. Liao, and K. Smedley, "State-plane analysis of regenerative snubber for flyback converters," *IEEE Trans. Power Electron.*, vol. 28, no. 11, pp. 5323–5332, Nov. 2013.

[17] Y. C. Kang, C. C. Chiu, M. Lin, C. P. Yeh, J. M. Lin, and K. H. Chen, "Quasiresonant control with a dynamic frequency selector and constant current startup technique for 92% peak efficiency and 85% light-load efficiency flyback converter," *IEEE Trans. Power Electron.*, vol. 29, no. 9, pp. 4959–4969, Sep. 2014.

[18] N. M. Mukhtar and D. D. Lu, "A bidirectional two-switch flyback converter with cross-coupled LCD snubbers for minimizing circulating current," *IEEE Trans. Ind. Electron.*, vol. 66, no. 8, pp. 5948–5957, Aug. 2019.

[19] H. Broeck, G. Sauerlander, and M. Wendt, "Power driver topologies and control schemes for LEDs," in *Proc. IEEE APEC* 2007, pp. 1319–1325.

[20] E. Serban, M. A. Saket, and M. Ordonez, "High-performance isolated gate-driver power supply with integrated planar transformer," *IEEE Trans. Power Electron.*, vol. 36, no. 10, pp. 11409–11420, Oct. 2021.

[21] G. Thiele and E. Bayer, "Current-mode LDO with active dropout optimization," in *Proc. IEEE Power Electron. Spec. Conf.*, Jun. 2005, pp. 1203–1208.